



How Well Can We Measure Galaxy Shapes with LSST? PSF Modeling for 3.2 Giga Pixels

M. J. Jee (UCD), J. A. Tyson (UCD), A. Connolly (U. Wash), J. Peterson (Purdue), D. Burke (SLAC), S. Kahn (SLAC), A. Rasmussen (SLAC), C. Claver (NOAO), D. Wittman (UCD), P. Gee (UCD), the LSST Collaboration

The focal plane of the LSST will be tiled with 189 4Kx4K CCDs, whose heights will vary less than 10 microns (peak-to-valley) in a complicated way relative to the nominal flat surface. Although this flatness deviation is small compared with other cameras, the small f-ratio of the LSST optics makes this focal plane flatness variation play a critical role in aberration-induced PSF elongation. In this poster, we present our simulation of the LSST PSF using the LSST optics model, the current specifications for the CCD assembly/fabrication, and the Cerro Pachón atmosphere model. As expected, we observe sharp discontinuities in PSF pattern across chip gaps, where abrupt changes in focus can happen. However, when we perform chip-by-chip PSF interpolation with basis functions derived from principal component analysis, these discontinuities do not prevent reconstruction of high-fidelity PSF models across the entire LSST focal plane. The resulting residuals in galaxy shear errors are well below that required for precision weak lensing for the LSST survey. We support this claim through image simulations with real galaxy images sampled from the HST/UDF data. Based on this work and related Subaru observations we make a projection of LSST cosmic shear systematic error and signal-to-noise ratio. With hundreds of dithered and rotated images of each sky patch in each optical band, the LSST focal plane non-flatness and atmosphere effects will produce residual shear correlation errors far below the cosmic shear signal over all angular scales of interest.

I. LSST FOCAL PLANE

We simulate the effect of the focal plane variation by creating the two-dimensional array that contains 189 4Kx4K CCD's height variation (worst case) and feeding the information to the ZEMAX model of the LSST optics.

Table 1. Focal plane height variation. Worst case scenario.

Factors	specification
entire focal plane	PV~10 μ m
raft height	PV~6.5 μ m
chip-to-chip height	PV~10 μ m
chip tilt	PV~2.5x10 ⁻⁴ rad
potato chip effect ¹	PV~5 μ m

1. 1~2 cycles within a CCD

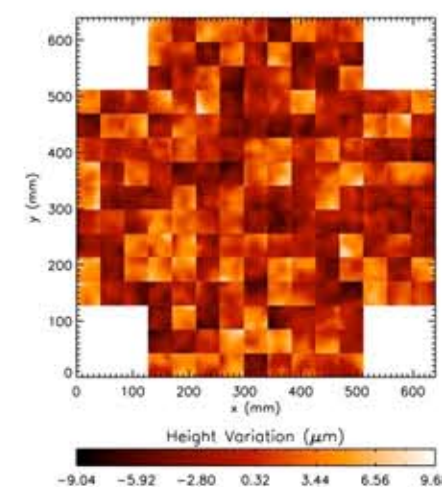


FIG 1. Simulated focal plane of LSST. We used the CCD assembly/fabrication specification in Table 1 to generate the LSST focal plane tiled by 189 CCDs.

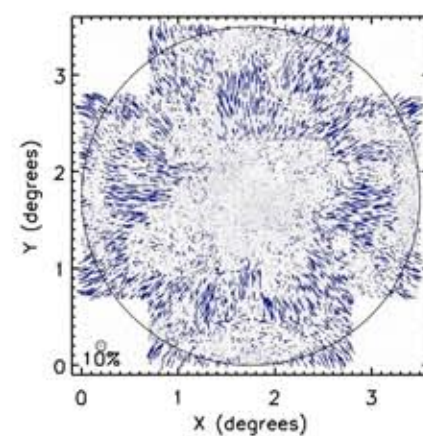


FIG 2. PSF Ellipticity distribution. We randomized the positions of 8000 virtual stars and ray-traced them through the optics.

Note the discontinuity of the height across the chip borders, which translates into the discontinuity of the PSF ellipticity. Although not shown here, the PSF width also changes abruptly across the chip borders. These systematics, unless corrected for, will introduce first order false signals in our gravitational lensing analysis using LSST.

II. ATMOSPHERIC TURBULENCE

The atmosphere above Cerro Pachón is modeled with six-layer Kolmogorov phase screens. We chose an outer scale of 20 m and a correlation length of 20 cm to randomize the phase screens. The highest layer at an altitude of ~15 km must have a physical width of at least ~1.5 km to cover the large LSST field of view and also to allow for wind-shifts during the simulated 15 s integration. The PSFs were sampled at an interval of 0.005 s for the above 8000 stars. For the details of the simulation setup, we refer readers to Jee et al. (2007b). We find that a typical PSF ellipticity of 0.01 was introduced during the 15 s exposure.

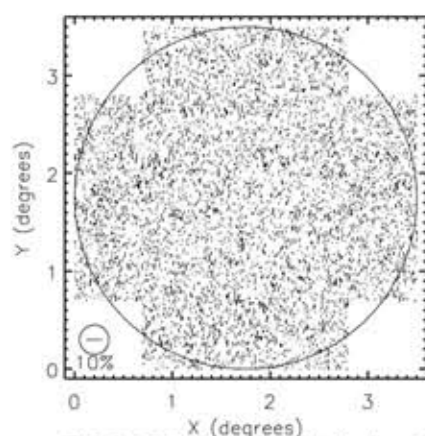


FIG 3. PSF Ellipticity distribution by atmospheric turbulence. Here we assume perfect optics and examine only the PSF ellipticity anisotropy due to the atmospheric turbulence. Note that we magnified the sticks by a factor of 4 with respect to the ones in Figure 2 because the atmosphere-induced ellipticity is relatively small (~0.01).

III. FINAL PSF AND CHIP-TO-CHIP MODELING

It is easy to imagine that the final PSF pattern will look somewhat like a diluted version of Figure 2 because the atmospheric turbulence is more likely to circularize the PSF than to introduce additional anisotropy to it. In the top panel of Figure 4 we display the final PSF ellipticity variation pattern, which is constructed by convolving the two sets of the PSFs shown in Figure 2 and 3. By and large, this expectation is correct; we observe that most of the outstanding features resemble those of Figure 2. However, it appears that the turbulence-induced ellipticity manifests itself where the optics-induced ellipticity is small (e.g., field center).

The discontinuous PSF pattern across the chip borders does not allow us to interpolate their variation with a single set of coefficients over the entire focal plane, which, however, was shown to work successfully in our previous work (Jee et al. 2007b) when no CCD height variation is considered

Here, we perform the interpolation only locally within each CCD. Due to the large number of CCDs, this of course complicates the PSF correction procedure substantially. Nevertheless, we found that this chip-by-chip PCA interpolation (Jee et al. 2007a) works very well (see the bottom panel of Figure 4) with as few as 20~30 stars per chip (allowing us to use only 2nd order polynomial interpolation). In real observations we expect to have >200 high S/N stars within a chip and thus the quality of the correction will further improve when the LSST is up and running. One way to quantify the level of the PSF correction accuracy is to examine the two-point correlation function of the PSF ellipticity, which we defer to Section VI.

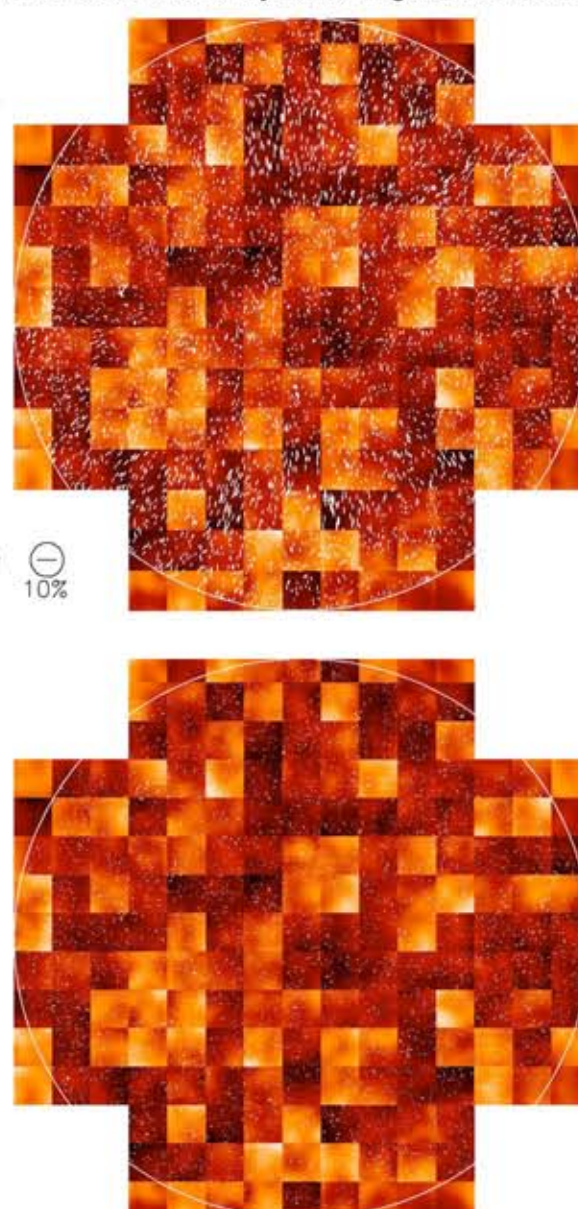


FIG 4. Final LSST PSF ellipticity pattern overlaid on top of the 189 CCD layout (top). The bottom panel displays the residual ellipticity pattern after we subtract the model constructed through chip-to-chip PCA.

IV. IMAGE SIMULATION

Does our good knowledge of the PSF always guarantee the bias-free measurement of galaxy shapes? Because the convolution by instrument PSF with noise is an irreversible process that inevitably destroys information, the galaxy shapes one obtains after seeing is in practice method-dependent even if one knows the exact PSF. To investigate how well we can determine galaxy shapes (thus gravitational shear) with the current level of the PSF modeling accuracy, we create simulated LSST images utilizing the publicly available Hubble Space Telescope (HST) Ultra Deep Field (UDF) images. The UDF images are so deep that a typical completeness limit is ~30 ABmag at the 10 sigma level, which is 2 mags deeper than the LSST's final co-added product.

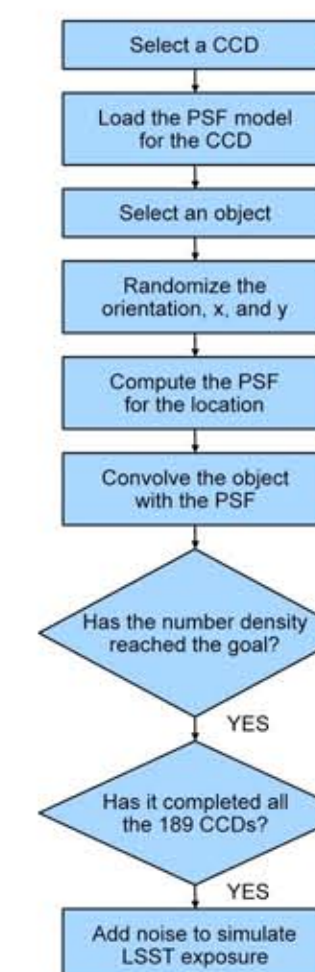


FIG 5. Flowchart of LSST image creation

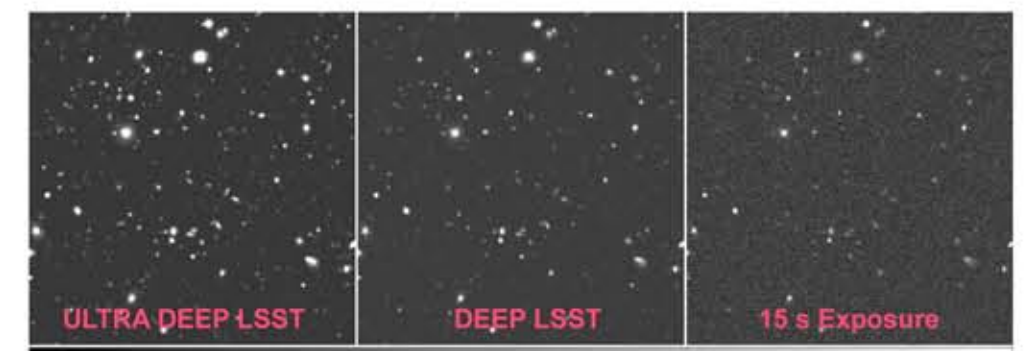


FIG 6. LSST image simulation. The "ultra deep" image has the same depth as the HST UDF. The deep and 15 sec exposure images reach about 28th mag (5sigma) and 24th mag, respectively.

V. GALAXY SHAPE MEASUREMENT

Objects are detected with SExtractor by searching for at least 12 connected pixels above 1.5 sky rms. We fit a PSF-convolved elliptical Gaussian to an object to determine its ellipticity. This scheme is identical to the technique proposed by Bernstein and Jarvis (2002) except that we perform the operation to the pixelated data rather than in the "shapelet" space.

VI. PSF SAMPLING AND RECOVERY

Stars are selected based on their size and magnitude. Unlike the case in Section III, these stars suffer from noise and neighbor contamination. Therefore, it is important to examine if the PSF sampling/interpolation with PCA used there still works here without manual intervention to remove potentially problematic outliers. Figure 7 shows that the reconstructed PSFs from the simulated images give a residual ellipticity correlation well below 10⁻⁷, which exceeds our goal for the LSST dark energy study via weak-lensing.

VII. HOW WELL CAN WE MEASURE GALAXY SHAPES?

Because we randomized the orientation of galaxies, the amplitude of our two-point shear correlation functions with galaxies must become vanishingly small (similar to the case of Figure 7) if the PSF is isotropic throughout the field. One might naively assume therefore that if our PSF modeling is perfect, the two-point correlation functions constructed from the psf-corrected galaxy ellipticity must be similarly consistent with zero. However, even if we use the exact PSF, the ellipticity measurements are still biased in the direction of the input PSF elongation. This bias is called "centroid bias" and has been noted in the literature (e.g., Kaiser 2000; Bernstein & Jarvis 2002). In brief, the centroid bias arises because galaxy centroid and ellipticity errors are on average larger in the direction of the PSF. This effect is subtle for large objects, but induces a significant bias for galaxies whose sizes approach those of the PSFs. Figure 8 shows the ellipticity histogram of galaxies (down to 28th mag) in the deep LSST image after correcting the PSF effect with the exact PSF. We can clearly see that the distribution still retains the significant memory of the input PSF ellipticity. However, this is not a fundamental barrier to the proposed LSST weak-lensing science. Because the bias is inversely proportional to the size of the objects, we can remove the bias by either applying an empirically-driven, size-dependent, formula to the ellipticity or using a modified (a bit more stretched than real) PSF in the elliptical Gaussian fitting. In Figure 9, we demonstrate that the two-point galaxy shear correlation function obtained in this way from a single deep LSST image (10 square degrees) is below 10⁻⁶. Because this noise floor is dominated by shot noise of the finite number of galaxies, and the statistical noise of the shear correlation function goes down as the inverse of the survey area (not as the inverse of the square root), the final 20,000 sq. degree data will enable us to achieve the proposed goal of the dark energy study via weak-lensing with the LSST. The results from the full-scale 20,000 sq. degree image simulation will be presented in future publications.

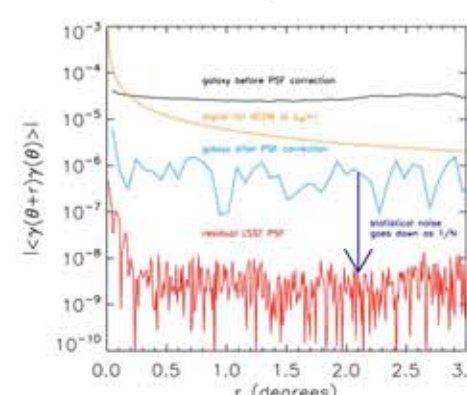


FIG 9. Residual 2-point shear correlation function from the simulated 10 sq deg final depth LSST image. Because galaxies are randomly oriented, this shows the background noise level in our cosmic shear measurement. Arrow shows the expected decrease for galaxies for 20,000 sq deg.

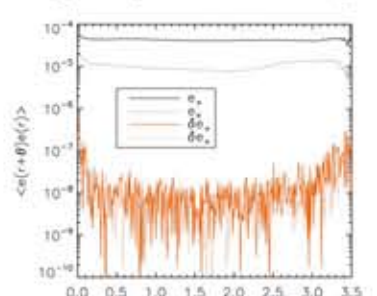


FIG 7. Ellipticity correlation of stars in the simulated 15 sec exposure LSST image.

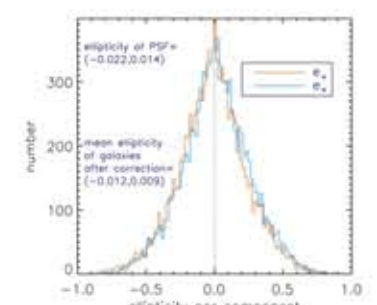


FIG 8. "Centroid bias" in ellipticity measurement even where the exact PSF is used. Note the horizontal shift between the two (e_y vs. e_x) distributions.

VIII. CONCLUSIONS

We have demonstrated that the current specification of the LSST and the analysis technique will enable us to reduce the systematics down to ~0.01% in the PSF ellipticity measurements. Our image simulation shows that this remarkable accuracy in the PSF modelling allows us to keep the background noise in the two-point shear measurement at ~10⁻⁶ or below in a single 10 sq. deg field. We expect that this noise floor will decrease linearly with the survey area until we reach the hard limit set by the PSF correction accuracy. A full-scale 20,000 sq. degree simulation is on-going, and a more robust PSF-correction (apart from PSF modelling) algorithm is under development.

REFERENCES

- Bernstein, G.M. & Jarvis, M. 2002, AJ, 123, 583.
Jee, M.J., Blakeslee, J.P., Sirianni, M., Martel, A.R., White, R.L., & Ford, H.C. 2007a, PASP, 119, 1403
Jee, M.J. et al. 2007b, Bulletin of the American Astronomical Society, 38, 983.
Kaiser, N. 2000, ApJ, 537, 555.